Quantum dynamics of wave packets in a Morse potential: A dynamical system approach

Prasun Sarkar,[1,*] Rohitashwa Chattopadhyay,[2,†] and Jayanta K. Bhattacharjee[3]
[1]*Indian Association for the Cultivation of Science, Jadavpur, Kolkata-700 032, India*
[2]*Department of Theoretical Physics, Tata Institute of Fundamental Research, Homi Bhabha Road, Colaba, Mumbai 400 005, India*
[3]*Department of Physics, Indian Institute of Technology Kanpur, Uttar Pradesh 208 016, India*

(Received 1 December 2023; revised 14 April 2024; accepted 9 August 2024; published 11 September 2024)

We show how a dynamical systems approach can, somewhat unexpectedly, be relevant in the quantum dynamics featuring oscillations and escape in the Morse potential. We compare the dynamics resulting from the approach with the results obtained from a direct numerical integration of the relevant Schrödinger equation to support our claim. An interesting finding of the numerical investigation is the marked increase in the probability of obtaining a significant fraction (more than 50%) of the wave packet in the classically forbidden range beyond a critical energy of the packet. The fact that the dynamical systems approach shows an instability near that critical energy is a definite indication of the relevance of dynamical systems to the quantum dynamics. At lower energies, the calculated mean position $\langle x\rangle$ and variance V from the dynamical system allow us to clearly establish the phenomenon of tunneling since the sum $\langle x\rangle + \sqrt{V}$ clearly exceeds, at various times, the classical bound on displacement for the corresponding energy.

DOI: 10.1103/PhysRevE.110.034207

I. INTRODUCTION

Studying quantum dynamics analytically, even in relatively simple potentials, is difficult. The dynamics that we are referring to is the time development of wave packets in time-independent potentials. In this paper, we will focus on Hamiltonians which cannot be split into a time-independent part of order unity and a small (generally time dependent) perturbation which can be handled by Fermi's golden rule. Our focus will be on the approximate techniques for time development of wave packets. Our approach complements the approximate techniques for time development introduced by Heller [1], exploiting the semiclassical limit. It was later followed up with particular emphasis on classically chaotic quantum systems [2–10]. An attempt at obtaining such a description was carried out for the free particle by Baird [11] and by Styer [12] for the simple harmonic oscillator. A different approach involving different order moments was introduced by Brizuela [13,14], exploiting the far-reaching potential of Eherenfest's theorem [15]. It was found that this reproduces [16] the exact solutions of wave-packet dynamics of free particles, particles in a simple harmonic potential, and also electrons with a spin-orbit coupling [17]. It was also possible to use this approach for anharmonic oscillators [18]. Further, for the nonlinear parametric oscillator, widely used for the signature of quantum fluctuations in nanomechanical oscillators [19–21], the dynamics of moments yields consistent answers [22]. An interesting extension of the semiclassical limit has been carried out by Goussev [23] and a third-order thawed-Gaussian approximation used by Kocia and Klales [24] yielded a treatment of nonlinearity in semiclassical dynamics. The generalized Gaussian wave-packet dynamics has been used very successfully by Pal *et. al.* [25] to explore the semiclassical limit of the kicked rotor.

Our goal in this paper is to introduce a dynamical system based formulation of the method of moments which holds at all energy scales and can address the quintessential feature of quantum dynamics—the phenomenon of tunneling. For this, we choose the Morse potential (Fig. 1), which plays a very important role in the binding of diatomic molecules. The Morse potential is

$$\phi(x) = \phi_0(e^{-2ax} - 2e^{-ax}). \tag{1.1}$$

In the above, a is an inverse length scale. Beyond this scale, the potential decays very fast. Recently, the Morse potential has also been used to study soft-matter systems [26–28] and small variants of it have been designed to study a wider range of molecules [29–31]. A classical particle in this potential with energy E ($-\phi_0 < E < 0$) will execute oscillations in the domain AB (see Fig. 1). The quantum particle with average energy E (this is a constant of motion in the quantum dynamics) will have a finite probability of being found outside the domain AB. Capturing this with the help of a dynamical system and comparing with the direct numerical simulation of the Schrödinger equation is the primary aim of our paper.

We discuss the formulation of the relevant dynamical system and its consequences in Sec. II. The results are compared with those obtained from a direct integration of the time-dependent Schrödinger equation in Sec. III. A brief conclusion is given in Sec. IV.

II. THE DYNAMICAL SYSTEM

We use the dynamics of an expectation value of an operator O. The time evolution is given by

$$i\hbar\frac{\partial}{\partial t}\langle O\rangle = \langle [O, H]\rangle, \tag{2.1}$$

*Contact author: prasuns25@gmail.com
†Contact author: rohitashwa.chattopadhyay@tifr.res.in

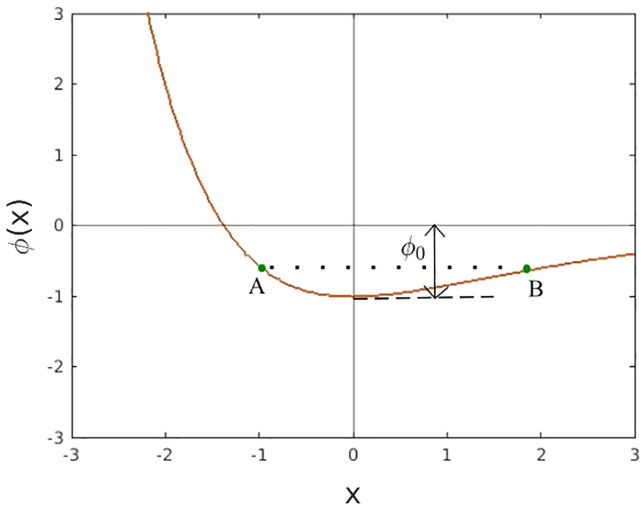

FIG. 1. The typical schematic diagram of a Morse potential, with $a = 0.5$ and $\phi_0 = 1$.

where H is the Hamiltonian of the system, which can be written as

$$H = \frac{p^2}{2m} + \phi(x). \tag{2.2}$$

We will subsequently set all energies E greater than $-\phi_0$ i.e., $0 > E > -\phi_0$. For the rest of this paper, we set $\hbar = 1$ and proceed with our analysis. We can now write the dynamics of the mean values of the position and momentum operators according to the procedure [4,16] introduced by Ehrenfest, which leads to the following dynamics in an arbitrary potential $\phi(x)$ for the mean position $\langle x\rangle$, the variance $V = \langle (x - \langle x\rangle)^2\rangle = \langle x^2\rangle - \langle x\rangle^2$, and the skewness $S = \langle (x - \langle x\rangle)^3\rangle = \langle x^3\rangle - \langle x\rangle^3 - 3\langle x\rangle V$. The mean acceleration comes from $\frac{d}{dt}\langle x\rangle = \frac{\langle p\rangle}{m}$ and $\frac{d}{dt}\langle p\rangle = -\langle \frac{d\phi}{dx}\rangle$ as

$$\frac{d^2\langle x\rangle}{dt^2} = -\frac{1}{m}\left\langle \frac{d\phi}{dx}\right\rangle. \tag{2.3a}$$

The dynamics of the variance is obtained from

$$\frac{dV}{dt} = \frac{1}{m}\langle xp + px\rangle - \frac{2}{m}\langle x\rangle\langle p\rangle$$

and another derivative yields

$$\begin{aligned}\frac{d^2V}{dt^2} &= \frac{d^2}{dt^2}(\langle x^2\rangle - \langle x\rangle^2)\\ &= \frac{2\langle (\Delta p)^2\rangle}{m^2} - \frac{2}{m}\left[\left\langle x\frac{d\phi}{dx}\right\rangle - \langle x\rangle\left\langle \frac{d\phi}{dx}\right\rangle\right],\end{aligned} \tag{2.3b}$$

where $\langle (\Delta p)^2\rangle = \langle p^2\rangle - \langle p\rangle^2$ represents the variance of the momentum. Similarly, the dynamics of the skewness can be obtained from

$$\begin{aligned}\frac{d^2}{dt^2}(\langle x^3\rangle - \langle x\rangle^3) = \frac{3}{m^2}\langle xp^2 + p^2x\rangle - \frac{6}{m^2}\langle x\rangle\langle p\rangle^2\\ - \frac{3}{m}\left[\left\langle x^2\frac{d\phi}{dx}\right\rangle - \langle x\rangle^2\left\langle \frac{d\phi}{dx}\right\rangle\right].\end{aligned} \tag{2.3c}$$

It is apparent that unless we have the potential $\phi(x)$ involving powers of x less than the cubic, the system cannot close. We can invoke closure by expressing the moment $\langle (x - \langle x\rangle)^n\rangle$ for $n \geqslant 4$ in terms of x, V, and S. We find that a very reasonable picture of the quantum dynamics can be obtained from the dynamical system described by the set of first-order equations leading to second-order equations of Eqs. (2.3a) and (2.3b).

It should be noted that the wave function $\psi(x,t)$—which is the solution of the time-dependent Schrödinger equation for a given Hamiltonian H—is a complex quantity that can be written as $\psi(x,t) = f(x,t)e^{i\eta(x,t)}$, where, $f(x,t)$ and $\eta(x,t)$ are real functions. The former is the amplitude and the latter the phase. The relation $\frac{dV}{dt} = \frac{\langle xp+px\rangle}{m} - \frac{2}{m}\langle x\rangle\langle p\rangle$ gives us, in one dimension, access to information about the phase of the wave function. It is important to write the average energy $E = \langle H\rangle$, which is a constant of motion for a time-independent Hamiltonian. From this relation, it follows that

$$E = \frac{\langle p^2\rangle}{2m} + \langle \phi(x)\rangle = \frac{\langle (\Delta p)^2\rangle}{2m} + \frac{\langle p\rangle^2}{2m} + \langle \phi(x)\rangle. \tag{2.4}$$

To find the quantum dynamics for any given potential $\phi(x)$, we need to specify an initial wave function $\psi_0(x)$ at time $t = 0$. This allows us to calculate all the moments at the initial instant and we can use them to evaluate the constants of integration as we track the evolution of the dynamical systems. In general, the initial wave packet will be taken to be $\psi_0(x) = \frac{1}{\sigma^{1/2}\pi^{1/4}}e^{-(x-\langle x\rangle)^2/2\sigma^2}e^{ikx}$. It gives a Gaussian probability distribution centered around $x = \langle x\rangle$ with width σ and momentum k. The calculation of moments as a function of time do not reveal the exact shape of the wave packet but gives a fair idea of what it looks like at later times. This is how the techniques of nonlinear dynamics can be used to extract useful information about the quantum dynamics.

We begin by discussing the dynamics for the particle in the Morse potential, as described in Eq. (1.1) when the energy E is close to (but greater than) $-\phi_0$. For later use, we define the quantity $\Delta E = (E + \phi_0)/\phi_0$, which is much smaller than unity when E is close to $-\phi_0$. The quantity ΔE equals unity when $E = 0$. For E close to $-\phi_0$ (or $\Delta E \ll 1$), we can expand the potential $\phi(x)$ of Eq. (1.1) as

$$\phi(x) = -\phi_0 + \frac{1}{2}\omega^2x^2 - \frac{\mu}{3}x^3 + \frac{\lambda}{4}x^4 + \cdots, \tag{2.5}$$

where $\omega^2 = 2\phi_0a^2$, $\mu = 3\phi_0a^3$, and $\lambda = 7\phi_0a^4/3$. Using Eqs. (2.3a)–(2.3b) and Eq. (2.4), we get

$$\frac{d^2\langle x\rangle}{dt^2} + \omega^2\langle x\rangle = \mu\langle x\rangle^2 - \lambda\langle x\rangle^3 + \mu V - 3\lambda V\langle x\rangle - \lambda S \tag{2.6}$$

and

$$\begin{aligned}\frac{d^2V}{dt^2} + 4\omega^2V =& 4\phi_0\Delta E - 2\omega^2\langle x\rangle^2 + \frac{4\mu\langle x\rangle^3}{3}\\ &+ 8\mu V\langle x\rangle + \frac{10\mu S}{3} - \frac{2\langle p\rangle^2}{m^2}\\ &- 2\lambda[K + 3S\langle x\rangle + 3V\langle x\rangle^2],\end{aligned} \tag{2.7}$$

where S is the skewness defined earlier and $K = \langle (x - \langle x\rangle)^4\rangle$ is the kurtosis of the distribution at any time. To write the dynamics of Eq. (2.3c) in terms of quantities already used, we need an approximation in the treatment of $\langle xp^2 + p^2x\rangle$ there.

We use the relation $E = \langle \frac{p^2}{2m} + \phi(x) \rangle$ to write Eq. (2.3c) to the lowest order as

$$\frac{d^2S}{dt^2} = 12\langle x\rangle\left[\frac{E}{m} - \frac{\langle p\rangle^2}{2m^2}\right] - 9\omega^2[S + 3V\langle x\rangle + \langle x\rangle^3] + 7\mu[K + 4S\langle x\rangle + 6V\langle x\rangle^2 + \langle x\rangle^4] - 3\mu[V^2 + 2V\langle x\rangle^2 + \langle x\rangle^4]. \quad (2.7a)$$

Neglecting μ,

$$\frac{d^2S}{dt^2} = 12\langle x\rangle\left[\frac{E}{m} - \frac{\langle p\rangle^2}{2m^2}\right] - 9\omega^2[S + 3V\langle x\rangle + \langle x\rangle^3]. \quad (2.8)$$

We note that the fixed point (i.e., stationary) value of $\langle p\rangle$ is zero and that of the variance is $V_0 = \Delta E/\omega^2$ from Eq. (2.7), working to the lowest order. Using these values, we find from Eq. (2.8) that the fixed point value of the skewness S is

$$S_0 = -5x_0(\Delta E)/3\omega^2. \quad (2.9)$$

Here x_0 is the fixed point value of $\langle x\rangle$ and for $\mu \leqslant 1$ (first departure from simple harmonic dynamics), $x_0 = \mu V_0/\omega^2$, and leads to a nonzero skewness. This is the major result coming from the low-energy dynamics and will be compared with the numerical solution of the Schrödinger equation dynamics carried out in Sec. III.

Treating the Morse potential as a set of anharmonic corrections on a simple harmonic form gives the significant result that the dynamics will acquire skewness even if one begins with a Gaussian wave packet. However, we anticipate that the dimensionless ratio $S_0/x_0^3 \ll 1$ and the inevitable skewness in the dynamics will be numerically small. We will see later that this fact is borne out by a numerical integration of the Schrödinger equation. Hence, at higher energies, where the full form of the potential is essential, we can make the assumption of the Gaussian shape being retained at all times and, accordingly, we consider the wave function to have the form

$$\psi(x,t) = \frac{1}{\pi^{1/4}\sigma^{1/2}} e^{-(x-\langle x\rangle)^2/2\sigma^2} e^{ik(t)x} = \frac{1}{(2\pi V(t))^{1/4}} e^{-(x-\langle x\rangle(t))^2/4V(t)} e^{ik(t)x}, \quad (2.10)$$

where $\langle x\rangle(t)$, $V(t)$ and $k(t)(= d\langle x\rangle(t)/dt)$ are the mean position, variance, and momentum at time t, respectively. We introduce the dimensionless variables $y = a\langle x\rangle$ and $u = 2a^2V$ along with a dimensionless time $\tau = ta\sqrt{2\phi_0}$ and use the above wave function in Eq. (2.10) to calculate the averages in Ehrenfest equations. The expectation values in Eqs. (2.3a) and (2.3b) are now evaluated to obtain the dynamical system,

$$\frac{d^2y}{d\tau^2} = \left[e^{(u-2y)} - e^{(\frac{u}{4}-y)}\right]. \quad (2.11a)$$

$$\text{and,} \quad \frac{d^2u}{d\tau^2} = \frac{\kappa}{2u} - 2u\left[2e^{(u-2y)} - e^{(\frac{u}{4}-y)}\right], \quad (2.11b)$$

where $\kappa = 2a^2/m^2\phi_0$ is the dimensionless control parameter (a measure of the quantum fluctuations relative to the strength of the Morse potential). However, we want the average energy (a constant of motion determined by the initial conditions) to be the relevant control parameter. Accordingly, we turn to Eq. (2.4) and using the wave function of Eq. (2.10) write it as

$$E = \frac{k^2}{2} + \frac{\kappa}{8u} + e^u - 2e^{u/4}. \quad (2.12a)$$

To make our calculations more tractable, we approximate the third and fourth terms on the right-hand side of Eq. (2.12a) with a single expression $-e^{-u/2}$ which is correct to $\mathcal{O}(u^2)$, i.e., for reasonably localized packets. Thus, we get

$$E \simeq \frac{k^2}{2} + \frac{\kappa}{8u} - e^{-u/2}, \quad (2.12b)$$

where k is the momentum of the wave packet. It must be mentioned that, without loss of generality, we set $m = 1$ and $\phi_0 = 1$ from Eq. (2.12a) for the rest of this paper. The averages have been carried out by using the standard definition: $\langle\hat{O}\rangle = \int_{-\infty}^{\infty} \psi^*(x,0)\hat{O}\psi(x,0)dx$ with $\psi(x,0)$ given by Eq. (2.4), where $\hat{O}$ is any observable such as the energy E or the potential ϕ. It must also be noted that for our system E as given by Eq. (2.4) is a constant of motion. Furthermore, approximating $e^u - 2e^{u/4}$ with $-e^{-u/2}$ is justified when $u < 1$. This is because when we expand $e^u - 2e^{u/4}$ and $-e^{-u/2}$ in a series, the terms up to first order in u are equal. The higher order terms would be smaller and thus can be neglected as long as $u < 1$. Substituting Eq. (2.12b) in (2.12b) for κ makes the evolution of u be governed by

$$\frac{d^2u}{d\tau^2} = 4\left[E - \frac{k^2}{2} + e^{-u/2}\right] - 2u\left[2e^{(u-2y)} - e^{(\frac{u}{4}-y)}\right]. \quad (2.13)$$

Between Eqs. (2.11a) and (2.13), we have a dynamical system controlled by dimensionless parameter $E' = (E - \frac{k^2}{2}) = -(|E| + \frac{k^2}{2}) = -\epsilon$. The magnitude of ϵ is less than unity in our range of interest.

To explore the dynamics, we need the fixed point of the system governed by Eqs. (2.11a) and (2.13). The stationary condition $\frac{d^2y}{d\tau^2} = 0$ for Eq. (2.11a) is

$$y_0 = 3u_0/4. \quad (2.14a)$$

Similarly, using the stationarity in Eq. (2.13), we get

$$u_0 e^{-u_0/2} = 2(-\epsilon + e^{-u_0/2}). \quad (2.14b)$$

The value of u_0 is found from the intersection of the two curves representing the two sides of Eq. (2.14b). We find the linearized equations around the stationary point as follows:

$$\frac{d^2(\delta y)}{d\tau^2} = e^{-u_0/2}\left[-\delta y + \frac{3}{4}(\delta u)\right] \quad (2.15a)$$

$$\text{and} \quad \frac{d^2(\delta u)}{d\tau^2} = 6u_0 e^{-u_0/2}(\delta y) - \left[\frac{\kappa}{2u_0^2} + e^{-u_0/2}\left(2 + \frac{7}{2}u_0\right)(\delta u)\right]. \quad (2.15b)$$

From here, we find the characteristic equation for the eigenvalues λ as

$$\lambda^2 + \left[e^{-u_0/2} + \frac{\kappa}{2u_0^2} + e^{-u_0/2}\left(2 + \frac{7}{2}u_0\right)\right]\lambda + \left[e^{-u_0/2}\left(\frac{\kappa}{2u_0^2}\right) + \left\{e^{-u_0}(2 + \frac{7}{2}u_0)\right\} - \frac{9}{2}u_0 e^{-u_0}\right] = 0. \tag{2.16a}$$

The eigenvalues around the fixed point are found to be

$$2\lambda = -\left[e^{-u_0/2} + \frac{\kappa}{2u_0^2} + e^{-u_0/2}\left(2 + \frac{7}{2}u_0\right)\right] \pm \sqrt{\left[e^{-u_0/2} + \frac{\kappa}{2u_0^2} + e^{-u_0/2}\left(2 + \frac{7}{2}u_0\right)\right]^2 - 4\left[e^{-u_0/2}\left(\frac{\kappa}{2u_0^2}\right) + \left\{e^{-u_0}\left(2 + \frac{7}{2}u_0\right)\right\} - \frac{9}{2}u_0 e^{-u_0}\right]}. \tag{2.16b}$$

From here, the condition for stability of the solution is found to be

$$\epsilon < \left[\frac{u_0}{4}\left(3 + \frac{7}{2}u_0\right) + 1\right]e^{-u_0/2}. \tag{2.17}$$

To conclude this section, we would like to mention that Eq. (2.13)—which is an approximation of Eq. (2.11b) via Eq. (2.12b)—was introduced to establish the energy E of the system as an appropriate control parameter. Having achieved this goal, from now on we will not be using the approximated Eq. (2.13). Instead, we will use Eq. (2.11b) along with Eq. (2.11a) in the subsequent section.

III. NUMERICAL RESULTS

In this section, we report results obtained via direct numerical integration of the time-dependent Schrödinger equation with a Morse potential. We start with an initial Gaussian wave packet and use the Crank-Nicolson algorithm [32] to obtain the wave packet $\psi(x,t)$ at later time t. Before implementing the algorithm, we need to specify the initial Gaussian wave packet. At time $t = 0$, we take the wave packet to have the form

$$\psi(x,0) = \frac{1}{\pi^{1/4}\sigma^{1/2}} e^{-x^2/2\sigma^2} e^{ikx}. \tag{3.1}$$

This packet has the initial expectation values $\langle x\rangle = 0$, $V = \langle x^2\rangle - \langle x\rangle^2 = \sigma^2/2$, and $\langle p\rangle = k$. From Eq. (2.12b), the average energy E for this packet is

$$\langle E\rangle = \frac{(1 + 2k^2\sigma^2)}{4\sigma^2} - e^{-a^2\sigma^2/2}. \tag{3.2}$$

In what follows, we will keep $\sigma = 1.0$, $a = 0.5$, and vary the total energy by varying the momentum k at $t = 0$. Our aim is to calculate the probability $P(x_0)$ of the particle staying within a distance x_0 of to the right of the origin using the time-dependent Schrödinger equation.

We consider the time-averaged effects, i.e., instead of considering the integral $P(x_0,t) = \int_{-\infty}^{x_0} |\psi(x,t)|^2\, dx$, we work with

$$P(x_0) = \lim_{T\to\infty} \frac{1}{T}\int_0^T dt \int_{-\infty}^{x_0} |\psi(x,t)|^2 dx. \tag{3.3}$$

Here, in Eq. (3.3) we have used $T = 10^5$ to produce our results in Fig. 2. Here, the choice of $T = 10^5$ is not critical as any large value of T will suffice, i.e., our results would not change if we use, say, $T = 15^5$ instead of $T = 10^5$. An essential feature of the quantum dynamics that we want to capture, by using the dynamical systems approach, is the issue of escaping from the potential well. This escape occurs in the dynamical system when the fixed point becomes unstable. For the Schrödinger equation description, this means that starting with an initial wave packet localized in the classical domain, we calculate the probability for finding the wave packet at a certain distance x_0 beyond the classical domain after a long time. We do this by numerically integrating the time-dependent Schrödinger equation to calculate the probability $P\ (x_0 = 4)$ defined in Eq. (3.3). The point $x_0 = 4$ is beyond the classical domain for all negative energies except those very close to $E = 0$, as can be seen from Fig. 1. Hence, a value of $P\ (x_0 = 4)$ close to unity implies that the quantum particle has not strayed too far from the classical domain, whereas $P(x_0 = 4) < 1/2$ certainly means that on an average the particle is far beyond the classical limit most of the time.

In Fig. 2, we show the probability of the particle being confined within the Morse potential as a function of the momentum k, which is a measure of the energy E of the particle.

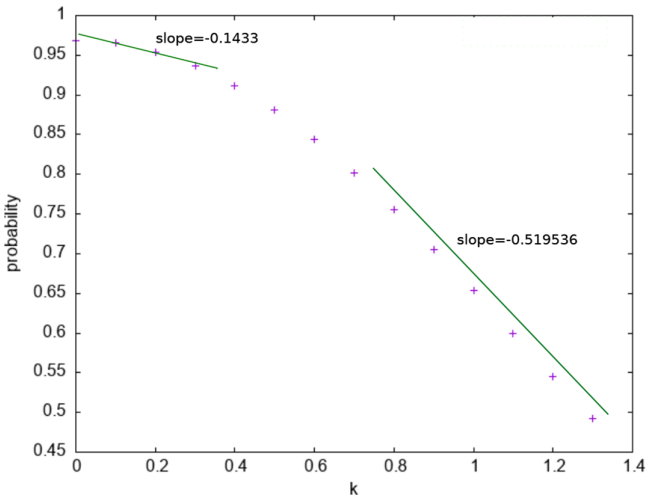

FIG. 2. The probability of the wave packet for staying within the position coordinate $x_0 = 4.0$, i.e., $P(x_0 = 4)$, has been plotted as a function of k. This plot is obtained by solving the time-dependent Schrödinger equation numerically (see text for details). We observe the slope increasing until about $k \simeq 0.8$ beyond which the slope is independent of k. We observe an analogous behavior—described in detail in the text—via our semiclassical approach using dynamical systems.

Here, in Fig. 2, a more negative value of the slope implies that the probability of staying within $x_0 = 4$ is decreasing more rapidly as we increase k. We see that in the initial stages the probability drops slowly as k is increased. This is true until around $k = 0.3$ and then there is a region where the slope changes with increasing energy and then becomes independent of energy at approximately $k = 0.8$. A transition happens in the quantum dynamics in the region $0.3 < k < 0.8$. In the subsequent paragraph, we will describe a corresponding behavior of the system using the dynamical systems approach.

To check for an analogous behavior with our semiclassical [33] setup using a dynamical system approach, we perform the following task. We solve the two coupled equations (2.11a) and (2.11b) numerically for the mean and variance. For a given set of parameters and initial conditions, the variables oscillate with finite amplitudes as shown in Figs. 3(a) and 3(b). However, there is a critical value of k between 0.77 and 0.78, beyond which the dynamical quantities $y = a\langle x\rangle$ and $u = 2a^2V$ start to diverge [Fig. 3(c)]. As mentioned above, in Fig. 2, the slope becomes independent of the energy at approximately around $k = 0.8$. Intriguingly, our semiclassical setup loses its stability at approximately the same value of k. Thus, we obtain a behavior analogous to *escape*, at the value of k between 0.77 and 0.78, via our dynamical systems approach. As soon as the fixed point becomes unstable, the dynamical system trajectory escapes to infinity. Since we have no control over the system anymore, a small variation of the initial condition (i.e., the energy) may lead to the particle escaping the potential from the right or left intersection point of the curve representing the Morse potential and the line corresponding to the constant energy. This is shown in Fig. 3(c), where, corresponding to two different initial conditions, the particle escapes from the right or left. Hence, in conclusion, the dynamical system, at this order, is capable of describing quantum tunneling till a critical value of k, beyond which more modes have to be introduced in the system to give a better description.

Additionally, we can go one step further and compute the time evolution of the Gaussian wave packet via the dynamical system approach and by direct numerical integration of Schrödinger's equation. Thus, the potency of our dynamical systems approach is brought out by comparing the evolution of the wave packet at every time step in the semiclassical and quantum domains. We set out by computing the mean and the variance of the Gaussian wave packet from the dynamical system description by numerically integrating Eqs. (2.11a) and (2.11b). From these two moments, we can reconstruct the Gaussian wave packet at each time step. Thus, we obtain the time evolution of the wave packet via our dynamical systems approach. We compare this result by obtaining the time evolution of the Gaussian wave packet from numerical integration of the Schrödinger's equation (see Supplemental Material [34]).

In the movies in the Supplemental Material [34], we tag the peak of both wave packets in each video (corresponding to $k = 0.1$ and $k = 0.5$). Let us denote the time period of the wave packet in Ref. [34], obtained via direct numerical simulation of the time-dependent Schrödinger equation, as T_{qm}. Let us also denote the absolute value of the difference in the time period of the two wave packets—obtained via semiclassical

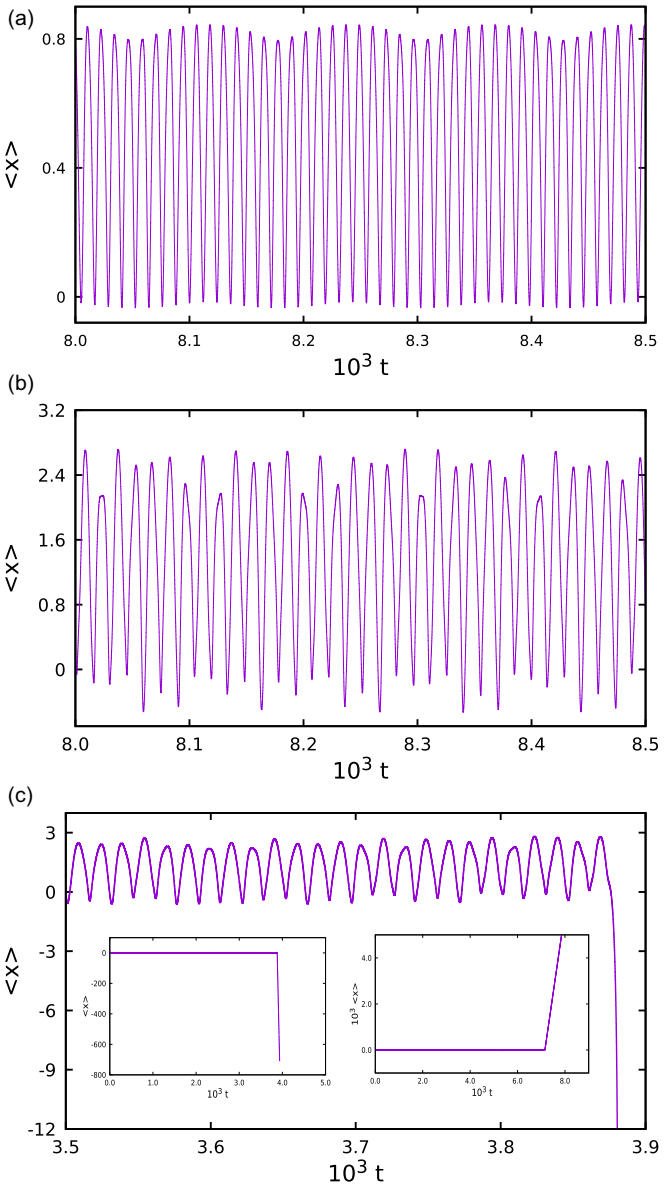

FIG. 3. (a) The variation of $\langle x\rangle$ as a function of time t has been shown for the momentum $k = 0.1$ corresponding to lower energy of the wave packet. This has been obtained by solving the coupled system as described in Eqs. (2.11a) and (2.11b), respectively. The maximum displacement is within the classical domain. (b) Same as in Fig. 3(a) but for the momentum $k = 0.77$ corresponding to higher energy of the wave packet. The higher energy leads to higher amplitudes of oscillations. (c) The variation of $\langle x\rangle$ as a function of time t blows up at $k = 0.78$. In this case, the particle escapes from the potential well. This gives us an estimation of the energy value of the particle, beyond which it escapes from the Morse potential. This k value is quite consistent with the results as obtained from the direct quantum mechanical analysis, as shown in Fig. 2. As observed in the two subpanels, the particle escapes towards the right of the potential (indicated by the subpanel on the right) when the initial mean $\langle x\rangle = 0$, while the initial variance $V = 0.72$ and the particle escapes towards the left (indicated by the subpanel on the left) when the initial mean $\langle x\rangle = 0$ and the initial variance $V = 0.74$.

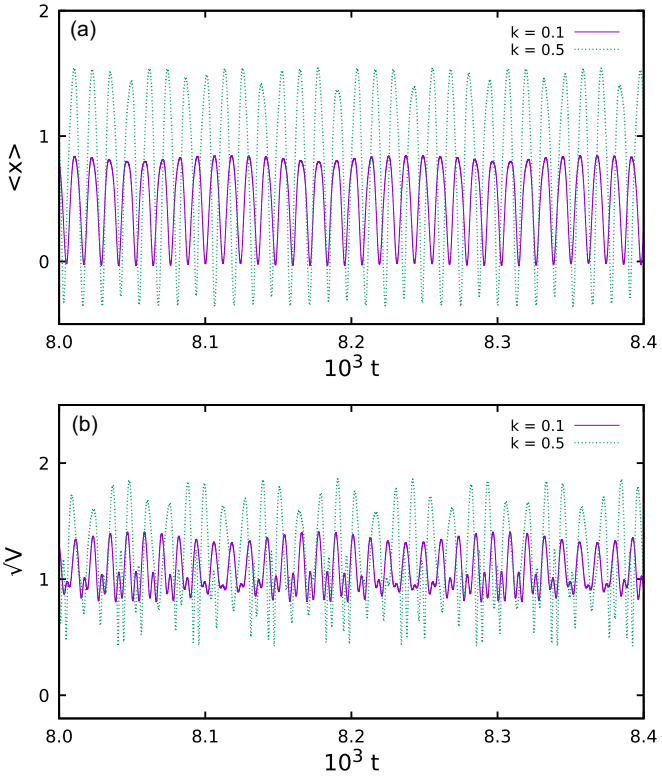

FIG. 4. (a) The oscillations of $\langle x \rangle$ as a function of time t has been shown for different values of k, as obtained from the dynamical system. The small oscillation (purple curve) one is for $k = 0.1$ and the large oscillation (green curve) one is for $k = 0.5$. The effect of changing k is moderate. (b) The oscillations of the square root of variance $\sqrt{V}$ as a function of time t for different values of k. The small oscillation (purple curve) is for $k = 0.1$ and the large oscillation (green curve) one is for $k = 0.5$. Note that the maximum value of $(\langle x \rangle + \sqrt{V})$ can be as large as 2.25 at $k = 0.1$, which corresponds to an energy of $E \simeq -0.6$. This is the maximum displacement that the particle can have from $x = 0$ at this energy. It can be seen from Fig. 1 that at $E = -0.6$, the range of the classical particle is less than 2, which makes the phenomena of quantum tunneling apparent in the dynamical system.

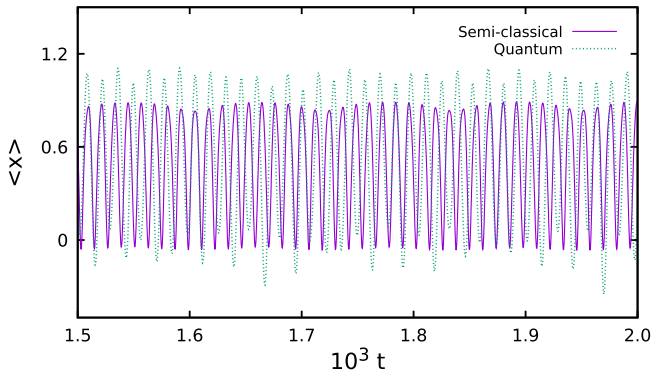

FIG. 5. The oscillations of $\langle x \rangle$ as a function of time t as obtained from the quantum mechanical consideration and the corresponding semiclassical results have been shown for a particular value of $k = 0.1$. This has been plotted here for a comparison between the semiclassical and quantum results. The solid line (purple) denotes the classical results while the dotted curve (green) is for the quantum mechanical results.

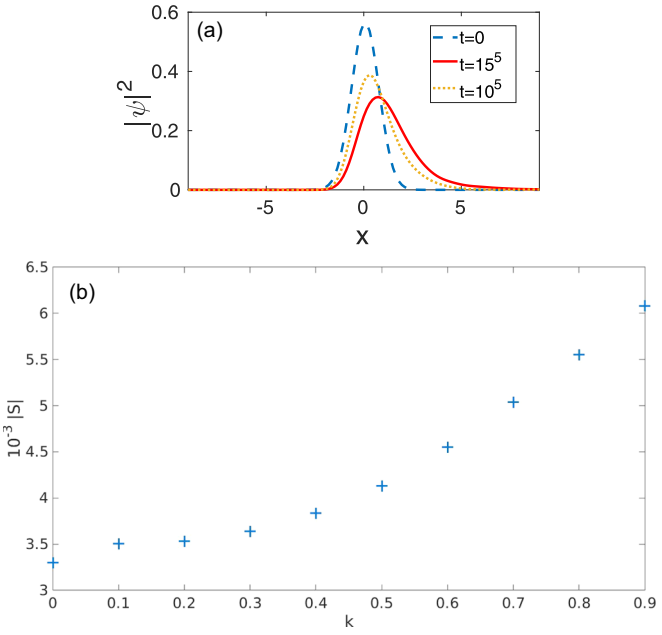

FIG. 6. (a) The probability $|\psi|^2$ has been plotted with respect to the position coordinate at different times. The time-evolved Gaussians are obtained by solving the time-dependent Schrodinger equation, in each cases. The wave packet has been released from the origin with $k = 0$. The blue one is observed at time $t = 0$, while the yellow one is being observed at later $t = 10^5$ time steps and the red one is at $t = 15^5$ time steps. We observe that significant skewness has not been developed, even after longer time. Thus, the assumption of ignoring the skewness in our analysis is justified, as mentioned in the text. (b) The skewness (S) has been plotted as a function of k (measurement of energy) values numerically from the quantum mechanical considerations. As can be seen, the increase is parabolic in k which is linear in ΔE and confirms the prediction of Eq. (2.9).

and quantum dynamics—for a particular value of k as $|\Delta t|$. We compute the quantity $|\Delta t|/T_{qm}$ for $k = 0.1$ and $k = 0.5$ to estimate how well our dynamical systems approach agrees with direct numerical simulations. From Ref. [34], we observe that $|\Delta t| = 4$ units when $k = 0.1$ while $|\Delta t| = 10$ units when $k = 0.5$. Furthermore, we obtain $|\Delta t|/T_{qm} \approx 0.06$ when $k = 0.1$ and $|\Delta t|/T_{qm} \approx 0.16$ when $k = 0.5$. The $|\Delta t|/T_{qm}$ value for $k = 0.1$ shows that the time period of the two wave packets does not differ by much. For $k = 0.5$, the value of $|\Delta t|/T_{qm}$ is greater than the value at $k = 0.1$. Still, the relative difference in the time period between the two wave packets when $k = 0.5$ is about 16%. This shows that our dynamical systems approach does a reasonably good job of approximating the dynamics of the wave packet over a range of k values, with the approximation being better at lower values of k.

We can further compare the two wave packets from Ref. [34]. To this end, let us denote the maximum displacement (from the origin and in the direction of the positive x axis) of the peak of the wave packet obtained via direct numerical simulations by X_{qm}. Let us also denote the absolute value of the difference in the maximum displacement (again from the origin and in the direction of the positive x axis) of the peak of the two wave packets —obtained via semiclassical and quantum dynamics—for a particular value of k as $|\Delta x|$.

We calculate the quantity $|\Delta x|/X_{qm}$ for $k = 0.1$ and $k = 0.5$. We find that $|\Delta x| = 0.13$ units when $k = 0.1$ while $|\Delta x| = 0.36$ units when $k = 0.5$. We also get $|\Delta x|/X_{qm} \approx 0.01$ when $k = 0.1$ while $|\Delta x|/X_{qm} \approx 0.03$ when $k = 0.5$. This again indicates that our dynamical system approach works well for a range of k values, with the approximation being better for low k values.

Further, we wish to explore the nature of oscillations of $\langle x\rangle$ and V as a function of time t for different values of k, from our dynamical system approach and establish that the data exhibits tunneling. Hence, we have plotted the required oscillations of $\langle x\rangle$ and V with respect to time for $k = 0.1$ and $k = 0.5$. In Figs. 4(a) and 4(b), we have plotted $\langle x\rangle$ and V as obtained from the dynamical system approach. We note that changing k is equivalent to changing the energy of the system. We now look at the values of $\langle x\rangle$ and V at the same instant of time from Figs. 4(a) and 4(b) and form the sum $(\langle x\rangle + \sqrt{V})$. It is clear from this analysis that at several instants of time this sum exceeds the bound of the classical domain[see the caption of Fig. 4(b)].

In Fig. 5, we compare the results obtained from the quantum mechanical consideration and the corresponding results obtained from our dynamical systems approach to check that how much our dynamical systems approach can capture the actual scenario, obtained from the quantum mechanical results. Thus, $\langle x\rangle$ has been plotted against time t for a particular value of $k = 0.1$. We observe that the frequencies of these two results matches reasonably well. However, there is difference in the amplitudes. The complete scenario of these two results have been shown in the movie, as described in Ref. [34].

We would like to end this section by discussing our results on the skewness that the wave packet develops. Furthermore, we would like to justify our assumption of ignoring the skewness in our semiclassical calculations on the basis of the results obtained from direct numerical simulation of the time-dependent Schrödinger's equation. In Fig. 6(a), we plot the skewness for $k = 0$ at different times. We notice that the skewness has not developed significantly even though the wave function is observed for long time intervals, such as 10^5 and 15^5 time steps. Thus, it justifies the assumption of ignoring the skewness in our theoretical analysis. In Fig. 6(b), we plot the skewness (S) as a function of k (measure of energy) numerically from the quantum mechanical considerations to show how the skewness develops with increasing energy of the wave packet. As anticipated, the skewness is small and increases linearly with ΔE [quadratic with k in Fig. 6(b)].

IV. CONCLUSION

In this paper, we have looked at the dynamics of a wave packet in a one-dimensional Morse potential from the usual quantum mechanical approach and also by writing a dynamical system involving the moments of different powers of the position operators. The dominant and unusual feature of the quantum dynamics is, however, the phenomena of tunneling. An unexpected feature, which our solution of the time-dependent Schrödinger equation for the Morse potential revealed, was the existence of a characteristic energy for which the tunneling probability of a particle, initially quite localized within the well of the Morse potential, suddenly increases. Interestingly, our technique of writing a dynamical system correctly shows a runaway instability at that energy. Below that energy, our dynamical system shows the expected behavior of the particle primarily oscillating about a shifted center and making excursions outside the classically allowed region. Consequently, we feel that the techniques used in the study of dynamical systems can be effectively employed for studying quantum dynamics.

All authors have contributed equally to this work and they declare no conflict of interest.

[1] E. J. Heller, J. Chem. Phys. **62**, 1544 (1975).
[2] A. K. Pattanayak and W. C. Schieve, Phys. Rev. Lett. **72**, 2855 (1994).
[3] A. K. Pattanayak and W. C. Schieve, Phys. Rev. E **50**, 3601 (1994).
[4] B. Sundaram and P. W. Milonni, Phys. Rev. E **51**, 1971 (1995).
[5] S. Chaudhuri, G. Gangopadhyay, and D. S. Ray, Phys. Rev. E **54**, 2359 (1996).
[6] L. E. Ballentine and S. M. McRae, Phys. Rev. A **58**, 1799 (1998).
[7] T. Bhattacharya, S. Habib, and K. Jacobs, Los Alamos Sci. **27**, 110 (2002).
[8] S. Habib, arXiv:quant-ph/0406011.
[9] V. Peano and M. I. Dykman, New J. Phys. **16**, 015011 (2014).
[10] S. Choi, R. Onofrio, and B. Sundaram, Phys. Rev. E **92**, 042907 (2015).
[11] L. C. Baird, Am. J. Phys. **40**, 327 (1972).
[12] D. F. Styer, Am. J. Phys. **58**, 742 (1990).
[13] D. Brizuela, Phys. Rev. D **90**, 085027 (2014).
[14] D. Brizuela, Phys. Rev. D **90**, 125018 (2014).
[15] N. Wheeler, *Remarks Concerning the Status and Some Ramification of Ehrenfest's Theorem* (Reed College Archives, Portland, Oregon, USA, 1998).
[16] A. Bhattacharyya, J. K. Bhattacharjee, and D. Sinha, Am. J. Phys. **89**, 627 (2021).
[17] V. Y. Demikhovskii, G. M. Maksimova, and E. V. Frolova, Phys. Rev. B **78**, 115401 (2008).
[18] R. Chawla and J. K. Bhattacharjee, Eur. Phys. J. B **92**, 196 (2019).
[19] T. P. Grozdanov and M. J. Raković, Phys. Rev. A **38**, 1739 (1988).
[20] S. Rahav, I. Gilary, and S. Fishman, Phys. Rev. Lett. **91**, 110404 (2003).
[21] H. Seok, E. M. Wright, and P. Meystre, Phys. Rev. A **90**, 043840 (2014).
[22] P. Sarkar and J. K. Bhattacharjee, Phys. Rev. E **102**, 052204 (2020).
[23] A. Goussev, Phys. Rev. A **96**, 013617 (2017).
[24] L. Kocia and A. Klales, Phys. Rev. E **94**, 032211 (2016).

[25] H. Pal, M. Vyas, and S. Tomsovic, Phys. Rev. E **93**, 012213 (2016).
[26] S. Zdravković, A. N. Bugay, and A. Y. Parkhomenko, Nonlinear Dyn. **90**, 2841 (2017).
[27] A. V. Bochkarev and A. I. Zemlyanukhin, Nonlinear Dyn. **104**, 4163 (2021).
[28] K. S. Sergeev, A. P. Chetverikov, and E. del Rio, Nonlinear Dyn. **102**, 1813 (2020).
[29] A. M. Desai, N. Mesquita, and V. Fernandes, Phys. Scr. **95**, 085401 (2020).
[30] C. A. Onate, I. B. Okon, U. E. Vincent, E. S. Eyube, M. C. Onyeaju, E. Omugbe, and G. O. Egharevba, Sci. Rep. **12**, 15188 (2022).
[31] S. Bhattacharjee and J. K. Bhattacharjee, J. Math. Chem. **50**, 1398 (2012).
[32] J. Crank and P. Nicolson, Math. Proc. Cambridge Philos. Soc. **43**, 50 (1947).
[33] When we refer to our approach via dynamical systems as semiclassical, we do not mean a semiclassical approach in the usual sense. In our case, the term semiclassical implies that we are using the Ehrenfest theorem along with some added approximations that enable us to ignore the higher moments (skewness, kurtosis, etc.) of the wave packet, whereas, typically in literature, a semiclassical approach implies that one is working with quantum dynamics in a high-energy regime.
[34] See Supplemental Material at http://link.aps.org/supplemental/10.1103/PhysRevE.110.034207 for enclosed video files showing the time evolution of the wave packet. The file titled video-k-0.1.avi shows the time evolution of the Gaussian wave packet—both semiclassical (red curve) and quantum (blue curve)—for $k = 0.1$. Similarly, the file titled video-k-0.5.avi shows the time evolution of the Gaussian wave packet—both semiclassical (red curve) and quantum (blue curve)—for $k = 0.5$. In both files, the semiclassical Gaussian wave packets (i.e., the red curves) are reconstructed from the calculated moments by using Eq. (2.10) in the text, while the quantum Gaussian wave packets (i.e., the blue curves) are obtained via direct numerical integration of the time-dependent Schrödinger equation. The black horizontal line parallel to the x axis in both files denotes the average energy corresponding to respective k values.